Structural Aspects of the Bis(2,2′-dipicolylamine)iron(II) Cation

RAYMOND J. BUTCHER
Chemistry Department, Howard University, Washington, DC 20059, U.S.A.
and ANTHONY W. ADDISON*
Chemistry Department, Drexel University, Philadelphia, PA 19104, U.S.A.

(Received August 16, 1988)

Abstract

The title complex crystallized as the BF_4^- salt in the orthorhombic space group $Fdd2$, with unit cell parameters $a = 21.749$ ($\sigma = 0.004$), $b = 27.788(0.006)$, $c = 8.900(0.002)$ Å. The iron(II) atom has slightly distorted octahedral coordination, in which the ligands are bound in a *cis-facial* configuration. The electronic properties of this brightly coloured low-spin complex are briefly discussed in relationship to the determined structure, and commentary is made upon the relationship between the lengths of Fe–N(aliphatic) and Fe–N(heteroaromatic) bonds in sexacoordinate iron(II) complexes and the spin state of the iron.

Introduction

Heterocyclic nitrogen donor and α-diimine complexes of iron(II) continue to receive considerable attention in the literature, principally because of the thermal spin-state equilibria ($S = 0 \rightleftharpoons S = 2$) which they often exhibit. These frequently cooperative equilibria have been studied occasionally in solution [1, 2], but more often in the solid state by techniques traditionally including magnetic susceptometry, optical [1, 2] and infrared [3] absorption spectroscopies and X-ray crystallography [4], and more recently, by these former techniques coupled with optical pumping of the complex into an allowed ligand-to-metal charge-transfer (LMCT) excited state which can relax into a long-lived metal spin-excited state [1, 3, 5].

We report here on the crystal and molecular structure of the iron(II) complex of the tridentate nitrogen donor ligand 2,2′-dipicolylamine (bis[2-pyridylmethyl]amine; Dipica) shown in Fig. 1, and note some other structure-related properties of this complex cation.

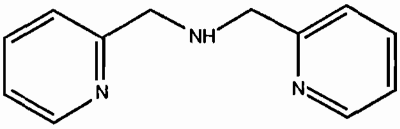

Fig. 1. The ligand Dipica.

Experimental

The complex was prepared by addition of a slight stoichiometric excess (Fe:Dipica = 1:2.1) of an aqueous ligand solution to aqueous iron(II) chloride tetrahydrate solution. The iron(II) solution contained ascorbic acid (*ca.* 5 mol.%) to reduce adventitious iron(III), and both solutions were continuously purged with N_2 gas during the procedure. Addition of excess sodium tetrafluoroborate led to a virtually quantitative yield of $[Fe(Dipica)_2](BF_4)_2$ as deep red prisms which were suitable for diffraction experiments.

Data were collected by standard methods on a Nicolet P3m microprocessor-controlled four-circle X-ray diffractometer operating in the θ–2θ mode with scans 1.2° above and below $K\alpha_1$ and $K\alpha_2$ of the Mo X-radiation monochromated with a graphite crystal at a wavelength of 0.71069 Å. The data were processed using standard routines. All non-equivalent reflection intensities for which $3.8° < \theta < 60°$ were collected. The intensities of four standard reflections monitored every 96 reflections showed no greater fluctuations than would be expected from Poisson statistics. The 2082 raw intensity data were corrected for Lorentz-polarization effects and absorption, and those 1065 reflections for which $I > 3\sigma_I$ were used in the final structural refinement. A three-dimensional Patterson synthesis was used to determine the heavy-atom positions, which phased the data sufficiently well to permit the location of the remaining non-hydrogen atoms from difference Fourier synthesis. Full-matrix least-squares refinement of the model was carried out as previously described [6], anisotropic temperature factors being introduced for all non-hydrogen atoms. Further difference Fourier calculations enabled the

---

*Author to whom correspondence should be addressed.

0020-1693/89/$3.50

location of the hydrogen atom positions, which were include in the refinement for four least-squares cycles and then held fixed. The model converged with R = 3.92% and R_w = 4.45%. A final Fourier difference map was featureless. Values for scattering factors and anomalous dispersion terms were taken from standard sources [7–9].

Results

The tetrafluoroborate salt crystallizes in the orthorhombic space group *Fdd*2, with unit cell parameters $Z = 8, a = 21.749$ $(\sigma = 0.004), b = 27.788(0.006)$, $c = 8.900(0.002)$ Å, $V = 5379$ Å^3, $\rho_{calc} = 1.561$ g cm^{-3}, $\mu = 6.391$ cm^{-1}.

Final atomic positional coordinates are listed in Table 1, while bond lengths and angles of significance are in Tables 2 and 3. An ORTEP drawing of the $Fe(Dipica)_2{}^{2+}$ complex ion is given in Fig. 2.

The low-spin iron(II) atom is essentially octahedral in coordination geometry, having the two ligands bound in the *facial* configuration. With its two five-membered chelate rings, each ligand apparently pinches together somewhat the three bonds of its corresponding octahedron face, so that the three N.Fe.N angles are each about 4°–8° less than the 90° ideal. The complex molecules are at positions of crystallographic C_2 symmetry, so there is no tendency toward trigonal prismatic geometry. All four five-membered chelate rings are in the 'envelope' conformation, with the picolyl–CH_2-carbon defining the apex of the 'flap'. There are two types of donor atoms: four heterocyclic nitrogens and two secondary aliphatic amino nitrogens: the C_2 symmetry is asso-

TABLE 1. Positional Parameters[a] and Isotropic Thermal Parameters[b]

Atom	x/a	y/b	z/c	B(Å^2)[c]
Fe	0.0000	0.0000	0.0000	3.41(1)
F1	0.1540(2)	−0.0059(1)	0.5158(9)	10.8(1)
F2	0.1565(2)	0.0544(2)	0.3545(6)	10.5(1)
F3	0.0664(2)	0.0298(2)	0.4518(5)	8.5(1)
F4	0.1359(2)	0.0673(2)	0.5969(5)	8.6(1)
N1	0.0051(2)	0.0547(1)	−0.1377(5)	4.08(9)
N1′	−0.0874(2)	0.0186(1)	0.0211(5)	4.2(9)
N2	0.0137(2)	0.0531(2)	0.1574(5)	5.0(1)
C1	0.0250(3)	0.0964(2)	−0.0743(8)	5.8(1)
C1′	−0.0996(2)	0.0513(2)	0.1278(6)	4.8(1)
C2′	−0.1593(3)	0.0685(2)	0.1524(8)	6.3(1)
C2	0.0192(4)	0.1401(2)	−0.1470(1)	9.2(2)
C3	−0.0068(4)	0.1423(2)	−0.2850(1)	11.4(2)
C3′	−0.2060(3)	0.0512(2)	0.0711(9)	6.7(2)
C4′	−0.1945(3)	0.0194(2)	−0.0436(9)	6.7(2)
C4	−0.0256(4)	0.1016(2)	−0.3437(9)	8.7(2)
C5	−0.0219(3)	0.0571(2)	−0.2725(7)	5.6(1)
C5′	−0.1335(3)	0.0028(2)	−0.0666(8)	5.4(1)
C6′	−0.0468(3)	0.0683(2)	0.2181(7)	6.0(1)
C6	0.0493(3)	0.0901(2)	0.0818(9)	7.0(2)
B	0.1283(3)	0.0365(2)	0.4793(8)	5.1(1)
H(N2)	0.0270(2)	0.0410(2)	0.2160(7)	6(1)*
H2′	−0.1630(2)	0.0930(2)	0.2030(7)	7(1)*
H2	0.0320(3)	0.1640(2)	−0.0900(1)	11(2)*
H3	−0.0210(3)	0.1670(3)	−0.3330(9)	11(2)*
H3′	−0.2460(2)	0.0700(2)	0.0970(7)	8(2)*
H4	−0.0500(2)	0.0970(1)	−0.3930(4)	1.4(7)*
H4′	−0.2180(2)	0.0080(2)	−0.1040(7)	6(1)*
H5	−0.0370(2)	0.0290(2)	−0.3030(7)	6(1)*
H5′	−0.1270(2)	−0.0210(1)	−0.1370(5)	4(1)*
H61′	−0.0450(2)	0.1060(2)	0.2150(6)	6(1)*
H61	0.0480(3)	0.1140(2)	0.1220(8)	9(2)*
H62	0.0930(2)	0.0790(2)	0.0720(6)	5(1)*
H62′	−0.0450(2)	0.0700(2)	0.3110(5)	5(1)*

*Starred items are refined isotropically. [a] Remaining atoms of the molecular unit are at (−x, −y, z). [b] e.s.d.s given in parentheses expressed *vs.* last significant digit. [c] Anisotropically refined atoms are given in the form of the equivalent isotropic thermal parameter: $4[a^2B_{11} + b^2B_{22} + c^2B_{33} + ab(\cos\gamma)B_{12} + ac(\cos\beta)B_{13} + bc(\cos\alpha)B_{23}]/3$.

TABLE 2. Bond Lengths (Å)

Atom 1	Atom 2	Distance	Atom 1	Atom 2	Distance	Atom 1	Atom 2	Distance
Fe	N1	1.957(5)	N2	C6	1.451(11)	C3'	C4'	1.374(13)
Fe	N1'	1.978(4)	N2	HN2	0.69(8)	C3'	H3'	1.04(8)
Fe	N2	2.057(6)	C1	C2	1.381(11)	C4'	C5'	1.421(10)
F1	B	1.343(9)	C1	C6	1.496(12)	C4'	H4'	0.80(6)
F2	B	1.363(9)	C1'	C2'	1.403(8)	C4	C5	1.391(11)
F3	B	1.382(7)	C1'	C6'	1.478(10)	C4	H4	0.71(4)
F4	B	1.362(8)	C2'	C3'	1.336(11)	C5	H5	0.88(6)
N1	C1	1.359(8)	C2'	H2'	0.83(7)	C5'	H5'	0.92(5)
N1	C5	1.338(9)	C2	C3	1.35(2)	C6'	H61'	1.05(6)
N1'	C1'	1.340(7)	C2	H2	0.91(11)	C6'	H62'	0.83(6)
N1'	C5'	1.345(8)	C3	C4	1.31(2)	C6	H61	0.75(8)
N2	C6'	1.485(10)	C3	H3	0.86(10)	C6	H62	1.01(6)

Numbers in parentheses are e.s.d.s in the least significant digits.

TABLE 3. Bond Angles (°)

Atom 1	Atom 2	Atom 3	Angle
N1	Fe	N1'	84.9(2)
N1	Fe	N2	82.0(2)
N1'	Fe	N2	83.5(2)
Fe	N1	C1	114.9(5)
Fe	N1	C5	125.1(5)
C1	N1	C5	118.1(6)
Fe	N1'	C1'	115.8(4)
Fe	N1'	C5'	125.1(4)
C1'	N1'	C5'	119.1(5)
Fe	N2	C6'	108.8(5)
Fe	N2	C6	105.6(5)
Fe	N2	HN2	103.0(7)
C6'	N2	C6	116.2(7)
C6'	N2	HN2	104.0(6)
C6	N2	HN2	118.0(6)
N1	C1	C2	121.7(9)
N1	C1	C6	113.4(6)
C2	C1	C6	124.7(8)
N1'	C1'	C2'	121.7(7)
N1'	C1'	C6'	116.6(5)
C2'	C1'	C6'	121.7(7)
C1'	C2'	C3'	119.8(8)
C1	C2	C3	120.2(9)
C2	C3	C4	117.0(9)
C3	C4	C5	124.0(1)
N1	C5	C4	118.5(8)
N1'	C5'	C4'	120.5(7)
N2	C6'	C1'	113.6(5)
N2	C6	C1	109.0(7)
N2	C6	H61	113.0(7)
N2	C6	H62	110.0(3)
C1	C6	H61	109.0(7)
C1	C6	H62	107.0(4)
H61	C6	H62	109.0(8)

The F–B–F angles range 108.3–110.0(0.7)°. Numbers in parentheses are e.s.d.s in the least significant digits. See also 'Supplementary Material'.

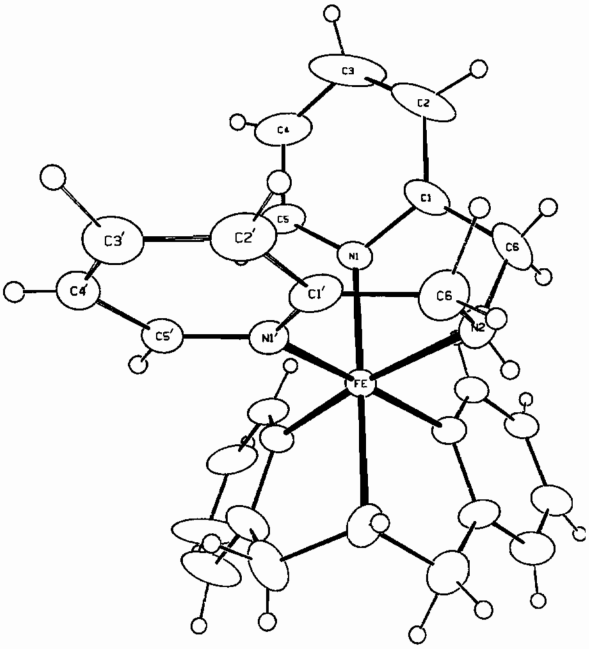

Fig. 2. ORTEP representation of the Fe(Dipica)$_2$$^{2+}$ complex ion.

ciated with a *cis*- rather than *trans*-configuration of the two central (amino) nitrogen donor atoms. There do not appear to be any unusual features associated with the ligands' structures; the pyridine rings of each ligand are canted at 72° to one another.

The BF_4^- anions are packed (Fig. 3) so that each of the two amino protons is only 2.29 Å from the fluorine atom of one of the two symmetrically disposed BF_4^- anions. The propensity of this NH unit for acting as an H-bond donor is probably related to the observed instability of the corresponding perchlorate salt in the solid state [1].

The two types of nitrogen atoms are associated with different Fe–N bond distances: the heterocyclic

TABLE 4. Some Representative Fe(II)–N Distances

Spin state	Mean N(het)	Mean N(sat)	Donor type(s)	Reference
Low-spin	1.956		terpyridyl	10
Low-spin	1.956		bipyridyl	11
Low-spin	1.970		phenanthroline	12
Low-spin	1.979	2.001	amine/pyridyl	13
Low-spin		2.089	Me_4cyclam	14
Low-spin		2.127	piperidine[a]	15
Low-spin	2.037		pyridine[a]	16
Low-spin	2.034		pyridine/thiazole	4
High-spin	2.250		triazole	17
High-spin	2.213		triazole	18
High-spin	2.193		triazole	18
High-spin		2.290	triazacyclononane	19
High-spin	2.229		pyridine	20
High-spin	2.170		pyridine	21
High-spin	2.223	2.181	picolylamine	22
High-spin	2.191		pyridine/thiazole	4
High-spin	2.120		pyrazine	23
High-spin	2.238		bipyrimidine	24
Intermediate-spin		2.165	Me_4cyclam	14

[a] Equatorial Fe–N(porphyrin) bonds excluded.

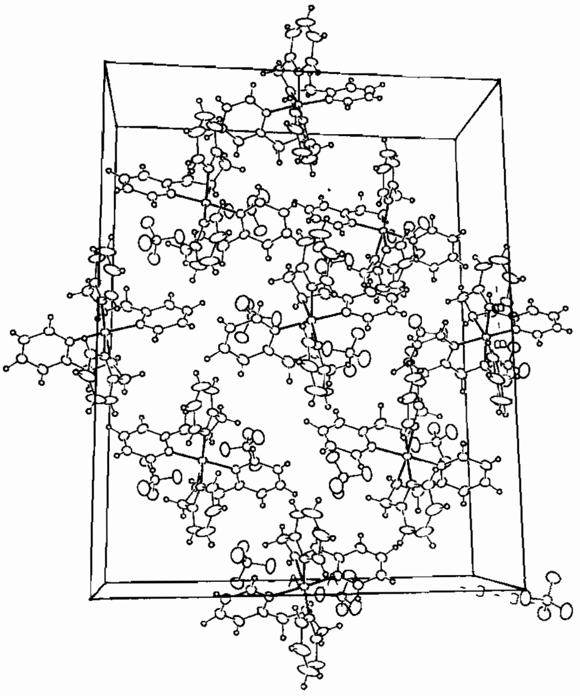

Fig. 3. View of the unit cell contents.

nitrogens are more closely bound, while the aliphatic nitrogens are about 5% more distant. This presumably reflects the sp^2 hydridization of the former, which may be associated with the $d\pi$–$p\pi$ overlap expected between metal and ligand in the C_2 point group. The low-spin character of the complex near 300 K was attributed to the presence of the more basic amino nitrogens, in comparison with other chelates with similar donor sets [1], but may be more subtly related to the ability of the pyridyl nitrogens to bond more closely because of the geometric attributes of this slightly flexible tridentate ligand. The Fe–N distances might be more satisfactorily contextualized by reference to Table 4, which contains representative data for sexacoordinate iron(II) with aliphatic and heteroaromatic nitrogen atoms. These have consistently confirmed that Fe–N distances are shorter in low-spin than in high-spin complexes (by about 0.2 Å). They also suggest generally that (i) in low-spin complexes, Fe–N_{het} linkages are about 0.05 Å shorter than Fe–N_{sat} ones, but (ii) less so in high-spin complexes (0.03 Å difference), while (iii) the Fe–N distances in an intermediate-spin ($S = 3/2$) complex are themselves intermediate in character. However, the pyridyl/amine coordination in the ambient temperature high-spin form of $[Fe(2\text{-picolylamine})_3]^{2+}$ may be exceptional; the N_{sat}–Fe distances are actually shorter than the N_{het}–Fe ones [22].

In the pertaining C_2 symmetry, the doubly occupied iron(II) d_{xy}, d_{xz} and d_{yz} orbitals transform as *a*, *b* and *b* respectively, while the four pyridyl π^*-based LUMO combinations will also transform as *a* and *b* representations. The electronic spectrum of the $Fe(Dipica)_2{}^{2+}$ cation exhibits a relatively intense band at 440 nm, proposed to be an LMCT transition [1]. Such absorptions had traditionally been considered to be associated only with the linking of an α-diimine moiety to iron(II) [25, 26]. There is no evidence that the exocyclic $-CH_2-NH-$ unit has become oxidized (to such an imine) during synthesis the atoms Fe, N2, C6, C6$'$ are not coplanar, and the C1.C6.N bond angles, for example are clearly closer to the sp^3 than sp^2 value. Moreover, a low-spin macrocyclic pyridyl iron(II) complex exhibits the same type of absorption band [13].

As a consequence of the low symmetry observed, all the possible $d \rightarrow \pi^*$ type LMCT electronic transitions are symmetry-allowed. The ligand-field strengths of the two types of donor atoms are quite similar, so although non-degenerate, the relevant ground and excited state manifolds are each expected to be closely internally collated in energy, and therefore no splitting of the relatively broad LMCT band is seen.

Supplementary Material

A complete list of bond angles is available from the authors on request.

Acknowledgements

We thank Drexel University for support, DOE, NSF and Howard University for X-ray equipment funding, and Nepera Chemical Co. for the gift of dipicolylamine.

References

1 A. W. Addison, S. Burman, C. G. Wahlgren, O. A. Rajan, T. M. Rowe and E. Sinn, *J. Chem. Soc., Dalton Trans.*, (1987) 2621.

2 L. J. Wilson and M. F. Tweedle, *J. Am. Chem. Soc., 98* (1976) 4825.

3 R. H. Herber, *Inorg. Chem., 27* (1988) 173.

4 A. T. Baker, H. A. Goodwin and A. D. Rae, *Inorg. Chem., 26* (1987) 3513.

5 S. Descurtins, P. Gütlich, K. M. Hasselbach, A. Hauser and H. Spiering, *Inorg. Chem., 24* (1985) 2174.

6 (a) C. B. Storm, C. M. Freeman, R. J. Butcher, A. H. Turner, N. S. Rowan, F. O. Johnson and E. Sinn, *Inorg. Chem., 22* (1983) 678; (b) J. T. Spencer, M. R. Pourian, R. J. Butcher, E. Sinn and R. N. Grimes, *Organometallics, 6* (1987) 335.

7 D. T. Cromer and J. T. Waber, *International Tables for X-ray Crystallography,* Vol. IV, Kynoch Press, Birmingham, U.K., 1974.

8 R. F. Stewart, E. R. Davidson and W. T. Simpson, *J. Chem. Phys., 42* (1965) 3175.

9 D. T. Cromer and J. A. Ibers, *International Tables for X-ray Crystallography,* Vol. IV, Kynoch Press, Birmingham, U.K., 1974.

10 A. T. Baker and H. A. Goodwin, *Aust. J. Chem., 38* (1985) 207.

11 M. E. G. Posse, M. A. Juri, P. J. Aymonino, O. E. Piro, H. A. Negri and E. E. Castellano, *Inorg. Chem., 23* (1984) 948.

12 A. Zalkin, D. Templeton and T. Ueki, *Inorg. Chem., 12* (1973) 1641.

13 L. Christiansen, D. N. Hendrickson, H. Toftlund, S. R. Wilson and C.-L. Xie, *Inorg. Chem., 25* (1986) 2813.

14 K. D. Hodges, R. G. Wollmann, S. L. Kessel, D. N. Hendrickson, D. G. Van Derveer and E. K. Barefield, *J. Am. Chem. Soc., 101* (1979) 906.

15 L. J. Radinovich, A. Bloom and J. L. Hoard, *J. Am. Chem. Soc., 94* (1972) 2073.

16 N. Li, P. Coppens and J. Landrum, *Inorg. Chem., 27* (1988) 482.

17 M. B. Cingi, A. A. M. Lanfredi, A. Tiripicchio, J. P. Cornelissen, J. Haasnoot and J. Reedijk, *Inorg. Chim. Acta, 127* (1987) 189.

18 M. B. Cingi, A. A. M. Lanfredi, A. Tiripicchio, J. Haasnoot and J. Reedijk, *Inorg. Chim. Acta, 101* (1985) 49.

19 J. R. Hartmann, R. L. Rardin, P. Chaudhuri, K. Pohl, K. Wieghardt, B. Nuber, J. Weiss, G. C. Papaefthymiou, R. B. Frankel and S. J. Lippard, *J. Am. Chem. Soc., 109* (1987) 7387.

20 G. J. Long and P. J. Clarke, *Inorg. Chem., 17* (1978) 1394.

21 G. J. Long, G. Galeazzi, U. Russo, G. Valle and S. Calogero, *Inorg. Chem., 22* (1983) 507.

22 L. Wiehl, G. Kiel, C. P. Köhler, H. Spiering and P. Gütlich, *Inorg. Chem., 25* (1986) 1565.

23 C. L. Klein, C. J. O'Connor, R. J. Majeste and L. M. Trefonas, *J. Chem. Soc., Dalton Trans.*, (1982) 2419.

24 A. Real, J. Zarembowitch, O. Kahn and X. Solans, *Inorg. Chem., 26* (1987) 2939.

25 R. J. P. Williams, *J. Chem. Soc.*, (1955) 137.

26 R. A. Palmer and T. S. Piper, *Inorg. Chem., 5* (1966) 864.